Proceedings of the 28th IEEE
EMBS Annual International Conference
New York City, USA, Aug 30-Sept 3, 2006

Magnetic Field Mapping by Selective Equipotential Excitation

Ouajdi Felfoul, S*tudent Member IEEE,* Michelle Raimbert, Sylvain Martel*, *Member IEEE*

NanoRobotics Laboratory, Department of Computer Engineering and Institute of Biomedical Engineering,
École Polytechnique de Montréal (EPM), Campus of the Université de Montréal, Montréal (Québec) Canada

*E-mail: sylvain.martel@polymtl.ca URL: www.nano.polymtl.ca

***Abstract*—A new magnetic field mapping method in MRI is presented. This technique is ideal for severe inhomogeneities where plane warp cannot be ignored. The present study employs a ferromagnetic ball to create a perturbation within the imaged volume. The magnetic moment and position of the device are acquired experimentally with a new technique that excites magnetic equipotentials within a volume. A three dimensional perturbation field is then reconstructed from which an accurate field map is acquired for any slice within the volume. This method is compared with phase imaging, which is commonly used to map the magnetic field perturbation. Preliminary investigations show that this method is accurate and provides field maps that do not suffer from distortion in the slice select and read direction. This method can help in the correction of susceptibility artifacts by providing an accurate map of the perturbing field generated by magnetic markers on medical instruments.**

***Index Terms*— MRI, field map, ferromagnetic, magnetic inhomogeneity, plane warp, susceptibility artifacts**

I. Introduction

Magnetic resonance imaging (MRI) is based on the application of linear magnetic field gradient superimposed on a uniform magnetic field. Generally, a field inhomogeneity of even 3.35 ppm, which is the mean chemical shift between fat and water, affects the image quality. If this variation is more important, more severe geometric and intensity distortions may be generated in the reconstructed images [1]–[6]. Correction requires knowledge of the magnitude and spatial extent of the magnetic field perturbation. This field map can be obtained either experimentally or theoretically, although, for the latter case, arbitrary geometries prove more difficult since no analytical equation describes the induced magnetic field.

Many MRI applications could benefit from magnetic field mapping in order to correct geometric distortions in images. For example, in interventional MRI a passive device exploiting susceptibility differences between markers and tissues is used. The marker material causes minimum distortion in conventional images yet enough signal void, or even signal enhancement, to be detected [7]–[9]. If the inhomogeneities, generated by the induced magnetic field of such markers, can be accounted for in the reconstruction process, the image quality could be improved. The same is true when imaging volumes containing a non ferromagnetic implant, stent or any foreign object with magnetic properties giving rise to susceptibility artifacts. Finally, field maps are useful in functional MRI where the images are very sensitive to magnetic field non-uniformities due to the long readout times of single shot acquisitions [10].

However, the field maps used to correct these encoding errors are often generated from images that also suffer from distortion. Phase images, for example, which are based on the subtraction of two successive phase acquisitions taken with different echo times [11], suffer from geometric distortion in the same way as conventional images acquired with a gradient echo based imaging sequence. This distortion occurs in both the slice select and readout direction, thereby producing an inaccurate field map. In fact, previous studies that use phase images to find the necessary correction, successfully correct for tissue-air interfaces but reported problems in the presence of a titanium implant [2].

II. Method

A. Magnetic source

In many applications, the dipole field equation can be used to describe the induced magnetic field. This is true with spherical shape and small object when the far field is considered. For our experiments we used a spherical shape, so, the induced magnetic field (B'), is described by Eq.1 where $\mu_0=4\pi 10^{-7}$ H·m^{-1} is the permeability of free space.

$$\vec{B}'(P)=\frac{\mu_0}{4\pi}\left(3\frac{(\vec{m}.\vec{r})\,\vec{r}}{r^5}-\frac{\vec{m}}{r^3}\right) \quad (1)$$

The dipolar magnetic moment $\vec{m}$ (A·m^2) is given by

$$\vec{m}=\frac{4}{3}\pi a^3\vec{M}\,, \quad (2)$$

where $\vec{M}$ is the saturation magnetization of the sphere (A/m).

B. Magnetic signature selective excitation

The selection of a particular slice in MRI is made possible because of the variation of the resonance frequency generated by the gradient magnetic field. In fact, the applied gradient for

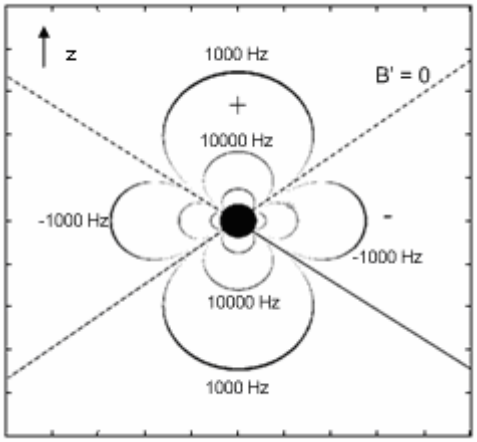

Fig. 1. MATLAB Simulation of the spatial distributions of the resonant frequency.

the slice selection modifies the resonance frequency in the readout direction according to the Larmor relationship. In the same way, the magnetic field created by the ferromagnetic object also modifies the frequency of the spins in the imaged volume. By using the properties of the dipole magnetic field generated by the ferromagnetic, a specific region in space is excited. By choosing the right frequency, a particular magnetic equipotential is excited as shown at Fig. 1. Two parameters control the excited volume; the excitation RF frequency and bandwidth. In Fig. 2 a bandwidth of 250Hz and frequencies of ±1000Hz and ±2000Hz are used to acquire the images.

C. Sequence

We used a modified spin echo sequence for imaging as depicted in Fig.3. The slice select gradient was removed and the frequency and the duration of the RF excitation signal were chosen according to the desired equipotential. A spin echo, as opposed to a gradient echo, sequence was chosen as it corrects for the dephasing caused by magnetic field inhomogeneities. SE sequence parameters were: T_R/T_E = 500/7.5 ms, FOV = 150×150 mm, with 256 sampled points in the read direction

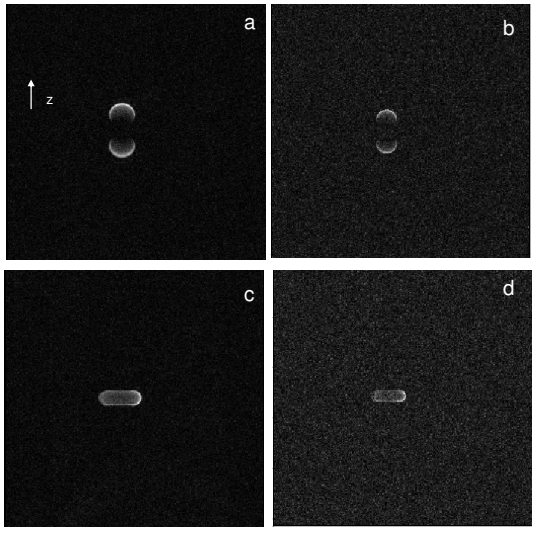

Fig. 2. MRI equipotential images taken with a bandwidh of 250 Hz and a frequency of (a) 1000Hz, (b) 2000Hz, (c) -1000Hz and (d) -2000Hz .

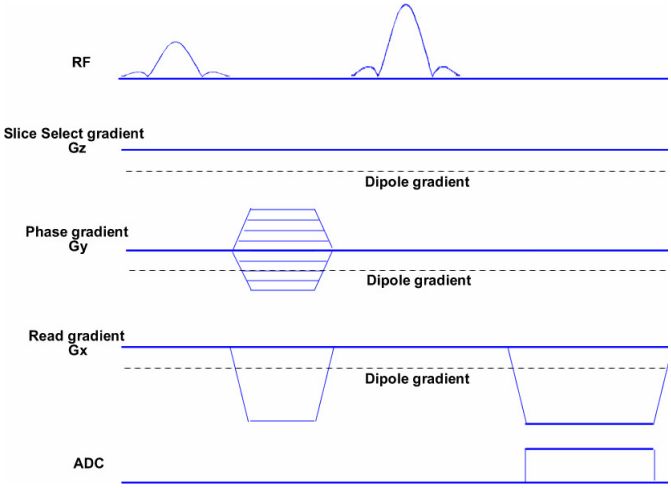

Fig. 3. Spin echo sequence used for imaging magnetic equipotentials.

and resulting in a pixel size of 0.59 mm. The entire volume of the phantom was filled with water mixed with 20 g/l gelatin, 1.25 g/l nickel sulphate, and 5 g/l NaCl, providing a solid homogeneous medium with short relaxation times. The ferromagnetic core used was a chrome steel sphere having a diameter of 1.5 and 0.8 mm.

D. Phase imaging

Phase imaging sequences generate a map of the perturbed magnetic field present during the encoding process. They show the magnetic field inside the imaged volume rather than its biological structure. Phase images of a ferromagnetic sphere (chrome steel, 0.8 mm diameter) were taken. Coronal images were acquired using a gradient echo mapping sequence run on a 1.5T Siemens Avanto MRI system with the following parameters: T_{E1} = 10 ms, T_{E2} = 14.76 ms, T_R = 500 ms, slice thickness = 2 mm.

E. Geometric distortions

In the imaging process, the dipole's magnetic field remains present during the readout encoding step as shown by the sequence diagram in Fig. 3. This background field causes the location of spins to be shifted along the read axis as a function of the field strength [12]. The perturbed encoded position is given by

$$x' = x + \frac{B'}{G_x}. \tag{3}$$

In Eq. (3), x' is the erroneous position of the excited spins located at x. The pixel shift is in the direction of the readout gradient. B' is the value of the dipole's magnetic field given by the RF excitation pulse, and Gx is the readout gradient along the x-axis. From Eq. 3, the only way to reduce the effect of pixel shifting, for a given offset excitation frequency, is by increasing the magnitude of the applied readout gradient. Therefore a realistic RF pulse, tuned to excite a wide range of magnetic field values, will result in a translation of every equipotential as given by Eq. 3. The behavior of the distortion is shown in Fig. 4. Due to the cubic dependence of the dipole's magnetic field, spins near the device experience a more pronounced shift than those further away.

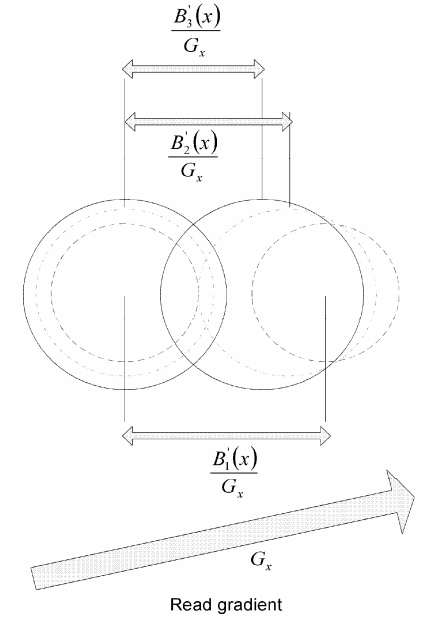

Fig. 4. Schematic view of the effect of the background gradient on the geometric encoding errors.

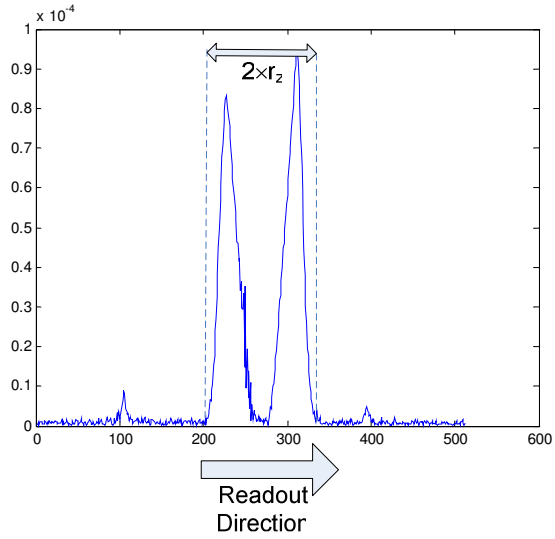

Fig. 5. Projection along the z-axis used to find the r_z value.

III. Results

A. Experimental magnetic field mapping

When imaging a magnetic equipotential a volume excitation is acquired. The spatial magnetic field cannot be extracted directly from the image. Instead, the location and the magnetic moment of the magnetic source can be found and used to generate a theoretical magnetic field map.

B. Magnetic moment measurement

Since the excitation RF frequency and bandwidth are known, then $B'(0,0,r_z)$ can be deduced. Having the value of the induced magnetic field in a particular location allow us to find the magnetic moment of the magnetic source. This is achieved by inverting Eq. 1 and considering only the z component of the magnetic field [12]. The MRI measured value of the magnetic moment was compared with measurements made by a Vibrating Sample Magnetometer (VSM) for two sphere diameters of 1.5 and 0.8 mm. Results are presented in Table I. In order to accurately estimate the magnetic moment of the sphere, the geometric shift must be accounted for and compensated.

TABLE I
MAGNETIC MOMENT MEASURED BY VSM AND BY MRI

	$\vec{m}$ measured by VSM (A·m^2)	$\vec{m}$ measured by MRI (A·m^2)	$\vec{m}$ measured by MRI corrected for geometric distortion (A·m2)
Sphere 1.5 mm	2.34E-3	3.10E-3	2.70E-3
Sphere 0.8 mm	3.63E-4	4.24e-4	3.29E-4

In this experiment the read gradient used was 14.5 mT/m. For an excitation frequency offset of 1000 Hz and a bandwidth of 1000 Hz the maximum geometric shift is 2.36 mm. The shift was transformed in pixel and substracted from the measured r_z value and then used to recalculate the corrected magnetic moment given in Table I.

C. Estimation of the magnetic field and phase imaging

A phase field map and an equipotential image were acquired with the sphere of 0.8 mm. The measured magnetic moment value was used to estimate the induced magnetic field. In Fig. 6, we show the reconstructed magnetic field map using our method and the phase image, both in the plane of the sphere.

IV. Discussion

These results show that magnetic equipotential excitation is a possible method for finding the magnetic moment of the device. The average error between the magnetic moment measured by MRI, after correcting for geometric distortion, and by VSM is 12 %. This is unexpectedly high and is most likely due to the method used to determine the distance between the source and a given equipotential, since it is not obvious which are the first pixels that belong to the signal. Very high resolution projections are desirable, in this case, to minimize this effect. In comparison with phase images, this method offers a way to bypass error that occurs in the read and slice select direction for high inhomogeneities. Furthermore phase images suffer from signal void in regions of large perturbation as it is seen in the center of the phase image (Fig. 6b), whereas mapping using equipotential excitation provides this information once the position and magnetic moment are determined. This method can be extended to experimentally find the magnetic field of an arbitrarily shaped object by exciting different equipotentials. However this will require an elaborate reconstruction method as the equipotential images are a 2D projection of a volume.

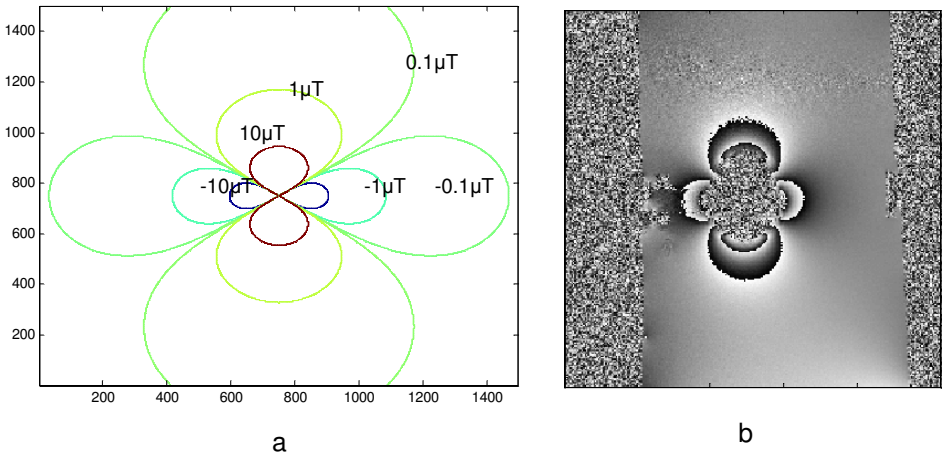

Fig. 6. (a) Reconstructed field map using equipotential excitation (b) field map acquired by phase image.

V. Conclusion

We introduce a new technique for mapping the magnetic field induced by a sphere. This method can be used in real time since we show that projections provide the necessary data to find the magnetic moment and the exact location of the sphere. Further study must be done to be able to accurately estimate the field induced by an arbitrary shape object. By doing so, we can accurately find the induced field from complex shape object such as metallic implant which increase the application field of this technique.

Acknowledgment

This project is supported in part by a Canada Research Chair (CRC) in Micro/Nanosystem Development, Fabrication and Validation, the Canada Foundation for Innovation (CFI), the National Sciences and Engineering Research Council of Canada (NSERC), and the Government of Québec. We acknowledge the support of Hospital Notre-Dame and Centre Hospitalier de l'Université de Montréal (CHUM) that provided the infrastructure necessary to conduct MRI tests.

References

[1] A. Glowinski, G. Adam, A. Bucker, J. van Vaals, and R. W. Gunther, "A perspective on needle artifacts in MRI: an electromagnetic model for experimentally separating susceptibility effects," IEEE Trans. Med. Imag., vol. 19, n. 12, pp. 1248-1252, Dec. 2000.

[2] A. Koivula, "Magnetic resonance image distortions due to artificial macroscopic objects". Ph.D. Dissertation, University of Oulu, Finland. 2002

[3] A. Ericsson, A. Hemmingsson, B. Jung, and G. O. Sperber, "Calculation of MRI artifacts caused by static field disturbances", Physics in Medicine and Biology, vol. 33, no. 10, pp. 1103-12, Oct, 1988

[4] C.J.G. Bakker, R. Bhagwandien, M. A. Moerland, and L. M. P. Ramos, "Simulation of susceptibility artifacts in 2D and 3D Fourier transform spin-echo and gradient-echo magnetic resonance imaging", Magnetic Resonance Imaging, vol. 12, no. 5, pp. 767-74, 1994.

[5] C. Nan-Kuei, A.M. Wyrwicz, "Removal of intravoxel dephasing artifact in gradient-echo images using a field-map based RF refocusing technique," Magnetic Resonance in Medicine, vol. 42, n. 4, pp. 807-812, Oct 1999.

[6] Z.H.Cho, Y.M. Ro, "Reduction of susceptibility artifact in gradient-echo imaging," Magnetic Resonance in Medicine;23:193–200, 1992

[7] R. van der Weide, C. J. G. Bakker, and M. A. Viergever, "Localization of intravascular devices with paramagnetic markers in MR images," IEEE Trans. Med. Imag., vol. 20, n. 10, pp. 779-785, Oct. 2001.

[8] J-H. Seppenwoolde, M. A. Viergever, and C. J. G. Bakker, "Passive tracking exploiting local signal conservation: The white marker phenomenon," Magnetic Resonance in Medicine, vol. 50, n. 4 pp. 784-790, Oct. 2003.

[9] O. Unal, F. R. Korosec, R. Frayne, C. M. Strother, and C. A. Mistretta, "A rapid 2D time-resolved variable-rate k-space sampling MR technique for passive catheter tracking during endovascular procedures," Magnetic Resonance in Medicine, vol. 40, n. 3, pp. 356-62, Sep. 1998.

[10] B.P. Sutton, D.C. Noll, J.A. Fessler, "Dynamic field map estimation using a spiral-in/spiral-out acquisition," Magnetic Resonance in Medicine, vol. 51, n. 6, pp. 1194-204, June 2004.

[11] E. Schneider, G. Glover, "Rapid in vivo proton shimming," Magnetic Resonance in Medicine,18:335–347, 1991.

[12] J.F. Schenck, "The role of magnetic susceptibility in magnetic resonance imaging: Magnetic field compatibility of the first and second kinds," Med. Phys. vol.23, no. 6, pp. 815-850, June, 1996.